Aspects of Diagenetic and Sequence Stratigraphic Framework on Reservoir Potential of Antalo Limestone, Mekelle Basin, Northern Ethiopia

Damenu Adefris [1, 4], *, M. E. Nton [2], O. A. Boboye [2] and Balemwal Atnafu [3]
[1] Petroleum Geosciences Program, Pan African University, Life and Earth Sciences Institute (including Health and Agriculture), University of Ibadan, Ibadan, Nigeria
[2] Department of Geology, University of Ibadan, Ibadan, Nigeria
[3] School of Earth Sciences, Addis Ababa University, P.O. Box 1176, Addis Ababa, Ethiopia
[4] Department of Geology, Debre Berhan University, P.O. Box 445, Debre Berhan, Ethiopia

ABSTRACT

The Mekelle Basin, located in the northern part of Ethiopia, is associated with the East African Mesozoic Rift Basins, and comprised Paleozoic to Mesozoic Formations which in most parts are hydrocarbon-bearing. The Antalo Limestone, a major lithostratigraphic unit, was investigated for its reservoir properties based on diagenetic features and direct porosity-permeability measurements from selected outcrop samples. Field evidences show that the limestone unit is extensive, fossiliferous, with karstic features such as caverns and caves, and inter-bedded with shale and sandstone beds. The associated fine-grained limestone beds are also characterized by condensed sections.

Four third-order depositional sequences, notably; DS1, DS2, DS3 and DS4, plus nine systems tracts based on facies staking patterns were delineated. The identified sequence boundaries included subaerial unconformity, transgressive and maximum flooding surfaces. Transgressive systems tracts (TST) of all depositional sequences comprised highly cemented facies of the outer-ramp to deep basinal environments, with absence of depositional porosity. Highstand systems tracts (HST) comprised coarse grained sand shoal facies, characterized by meteoric to marine phreatic cementation and dissolution porosities such as caverns and molds. Very low porosity (<0.5 – 4.6%) and permeability (<0.01 mD) values of some samples also indicated the impact of cementation. The lowstand systems tracts (LST) comprised tidal flat to lagoonal facies with caves, caverns and solution- enlarged fracture porosities. Within the LST, a sample with a relatively fair porosity (6.5%) and 0.91 mD permeability confirmed the presence of beds with capacity of storing fluids. Arising from evidences of dissolution porosity, the lowstand systems tract of the second depositional sequence (DS2) and the highstand systems tract of the fourth depositional sequence (DS4), the Antalo Limestone has some reservoir potential.

Keywords: Antalo Limestone, Mekelle Basin, Diagenesis, Sequence stratigraphy, Reservoir.

INTRODUCTION

The world's oil and gas resources are extracted, mainly from sandstone and carbonate reservoir rocks (Ehrenberg and Nadeau, 2005; Ahr 2008). The Ethiopian Ministry of Mines (EMoM, 2011) reported, that the Antalo Limestone of the Mekelle Basin, the shale and black limestone inter-beds, could serve as very good potential source rock.. However, the nature of the Antalo Limestone as a potential source and reservoir rock is not well understood. Equivalent units in East African, and other Mesozoic sedimentary basins in the region, have very good source and reservoir potentials (Carrigan *et al.,* 1995; Hunegnaw *et al*., 1998; Hakimi *et al.,* Hakimi *et al.,* 2012. According to Hunegnaw *et al*., 1998; the grainstone/packstone and dolomite facies in the Upper Hamanlei Formation of the contiguous Ogaden Basin in Ethiopia, are potential reservoirs with maximum porosity of about 23% and permeability values of 1000 mD. The characterization of reservoir potential for carbonate rocks, is highly dependent on evaluating the depositional history, diagenetic evolution, as well as sequence stratigraphic framework; sequences and systems tracts . Sequence stratigraphic analysis, particularly helps in subdividing the unit into different depositional sequences and systems tracts which can be used to interpret the prevailing allogenic and autogenic controls on sedimentation and post-depositional modifications . Therefore, this study is intended to investigate the diagenetic features and sequence stratigraphic framework as well as to ascertain

This work was funded by the African Union. The authors would like to thank Misters Akebom Teame and Berehanu Mebrehatu for their immense contribution during the field data collection. The authors are indebted to the Department of Geology, University of Ibadan. The authors are grateful to Nigerian Association of Petroleum Explorationists (NAPE) for the opportunity to present aspects of this study at the 38th Annual International Conference and Exhibition, Lagos, Nigeria.

by porosity-permeability measurements, the reservoir potential of the unit.

GEOLOGICAL SETTING AND STRATIGRAPHY OF THE MEKELLE BASIN

Sedimentary rocks cover a significant portion of Ethiopia with very thick Paleozoic – Mesozoic clastic, evaporite and carbonate formations in the Ogaden, Blue Nile, Mekelle, Gambela and South Omo Basins (Worku and Astin ,1992; Russo et al., 1994; Tefera *et al.,* 1996; Bosellini *et al.,* 1997; Hunegnaw *et al.,* 1998; Bosellini *et al.,* 2001; Gani e*t al.,* 2008) (Figure 1). The Mekelle Basin covers about 8,000 km2 comprised, mainly Paleozoic to Mesozoic sequences (Figure 2). These sequences are successively from oldest to youngest; Enticho Sandstone, Edaga Arbi Glacials, Adigrat Sandstone, Antalo Limestone, Agula Shale and Amba Aradam Sandstone (Beyth, 1972; Bosellini *et al.,* 1997) (Figure 3). The basin is considered an intracontinental sag basin formed as a result of cooling and thickening of a juvenile sub-continental lithospheric mantle and subsequent subsidence. (Alemu *et al.,* 2018). It is also characterized by a northwest – southeast trending normal fault systems commonly known as the Mekelle Outlier faults (Arkin *et al.,* 1971) that highly affected the sedimentary sequence and exposed in some places in the form of fault margin cliff exposures.

Basement rocks

The metamorphic terrain of northern Ethiopia, is part of the Arabian Nubian Shield (ANS) and characterized by thick volcano-sedimentary assemblages, that comprise metavolcanic rocks (Tsaliet Group), metasediments (Tambien Group), granitoid and mafic-ultramafic suites, with associated faults and shear zones (Arkin *et al.,* 1971; Beyth, 1972; Beyth *et al;* 2003; Asrat *et al;* 2004).

Enticho Sandstone and Edaga Arbi Glacials

These sedimentary sequences of the Mekelle Basin, are about 300 meters thick, which unconformably overly the Precambrian basement rocks, with a Cambrian – Upper Ordovician unconformity (Arkin et al; 1971; Tefera et al., 1996; Bussert and Schrank, 2007; Bussert, 2010).

Adigrat Sandstone

It is about 300 – 650 meters thick with variable colors and textural features, comprising white, yellow, brown to red, poorly to well sorted, fine-coarse grained sandstone with inter-beds of siltstone and clay (Arkin *et al.,* 1971; Beyth, 1972; Beyth *et al;* 2003; Bosellini *et al.,* 1997). It is considered to have a very good reservoir potential (EMoM, 2011).

Antalo Limestone

It has about 740 meters maximum thickness, dominated mainly by cliff-forming yellow, white to black limestone with significant inter-beds of marl, lenses of chert, and cross-bedded sandstone that comprises different types of fossils and some indicators of post-depositional processes such as karsts, channels, and caves (Beyth *et al;* 2003; Bosellini *et al.,* 1997). Moreover, Bosellini *et al.* (1997) studied this unit from the sequence stratigraphy point of view and interpreted as deposited in a ramp environment due to a transgression event that commenced in Late Jurassic. Oxfordian – Kimmeridgian age has been assigned to this limestone unit (Merla and Minucci 1938), Getaneh and Valera (2002) interpreted a shallow seawater depositional environment based on REE and major elements of non-carbonate constituents. Detailed microfacies and stable oxygen and carbon isotopes analyses, also showed shallow to deep marine environments and meteoric–marine phreatic cementations, and deep-burial diagenesis ((Adefris *et al.,* 2020) Kiessling *et al.* (2011)) studied marine benthic invertebrates (such as corals, brachiopods, and bivalves), from the Antalo Limestone and assessed their biogeographic patterns to deduce the Callovian to Kimmeridgian paleogeography of Ethiopia. The results showed that Ethiopia was part of the Late Jurassic shelf environment, facing the Tethys Sea.

The associated brown shale and black limestone inter-beds in this unit are considered as very good source rocks (EMoM, 2011).

Agula Shale

It is about 60 – 250 m thick, which comprises gray, green and black shale, marl and clay subunits with inter-laminae of black limestone, gypsum, and dolomite (Arkin *et al.,* 1971; Beyth, 1972; Bosellini *et al.,* 1997). It could have very good source rock potential (EMoM, 2011).

Amba Aradam Sandstone

The Amba Aradam Sandstone conformably overlies the Agula Shale, with thickness ranging from 60 meters to 200 meters (Arkin *et al.,* 1971; Beyth, 1972). It is considered to be a very good reservoir rock in the basin.

Igneous rocks

These rocks cover the country's highland plateau (Ayalew and Yirgu, 2003), which, in northern Ethiopia, have been subdivided into lower and upper sequences based on variation in their composition (Kabeto, 2010).

MATERIALS AND METHODS

Field Sampling and Analytical Methods

Fieldwork was conducted through outcrop description, section logging, and sample collection. A total of ninety-two (92) rock samples were collected from three outcrop locations, representing the full thickness of the unit. Different layers of rocks were described and measured, starting from bottom to top of the sections. This was done on the bases of lithological differences in composition,

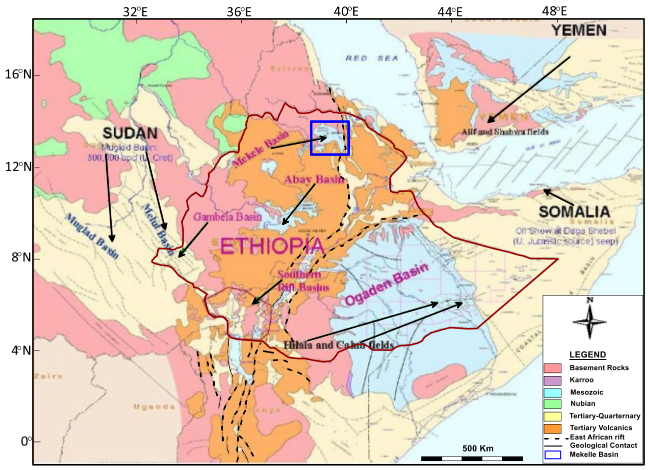

Figure 1: Geologic map showing the locations of hydrocarbon prospective sedimentary basins of Ethiopia and potential oil fields of Sudan, Somalia, and Yemen (After EMoM, 2011).

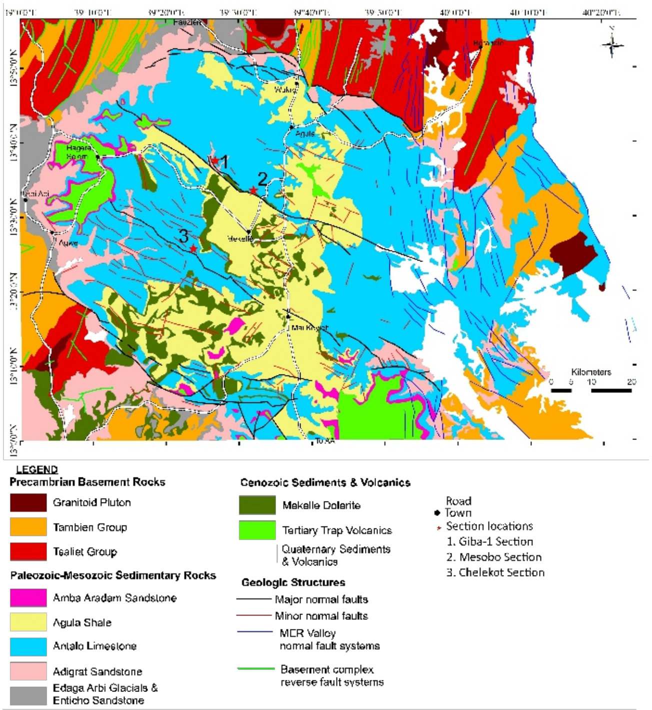

Figure 2: Geological map of the Mekelle Basin and location of the studied sections (After Arkin *et al.,* 1971).

color, texture, fossil content, and sedimentary structures. Fresh and representative rock samples, made up of fine grained and skeletal limestones and sandstone were collected. The collection of samples was, generally, carried out within five-meter intervals. However, several samples were collected, where a number of facies types encountered within short intervals. However, in some of the sections, where single facies type predominates, samples were taken at large intervals.

Thin Section Petrography

A total of 92 samples made up of limestone and sandstone were used for thin section preparation by standard methods. Thin sections were prepared using a *GEOFORM Precision* Thin Section Cutting and Grinding Machine and a *Kemtech III* Geological Lapping Machine. The sandstone samples were impregnated, with a resin to lithify and harden the samples and make a safe thin section cutting. Petrographic analysis of thin sections was carried out on all of the collected samples to identify different microfacies types and diagenetic features, using a monocular polarizing petrographic microscope. The identification, analysis, classification, and visual estimation of different porosity types were carried out using point counting. The preparation, microscopic examination and photomicrography of thin sections were done in the petrography laboratory, Department of Geology, University of Ibadan, Ibadan, Nigeria.

Porosity Measurement

More detailed and direct measurement and analysis of porosity and permeability were carried out on eight (8) limestone samples, selected from each depositional sequence of the unit. Before measurements, samples were cleaned of surface dust contamination. Sample weights were measured using a self-contained precision balance, calibrated to an accuracy of ± 0.001 g. The samples were dried and allowed to cool in a desiccator. The samples were then placed into the *VINCI HePLEX®* helium porosimeter matrix cup, for grain volume determination. Porosity was measured using a porosimeter, with Helium gas of 200 Pa (Pascal) reference pressure and applying Boyle Mariotte's law.

Permeability Measurement

The samples were placed into the VINCI PoroPerm core holder for permeability determination at a steady state. Permeability was measured using a permeameter, with nitrogen gas at 400 Pa of confining pressure applied to the sample and applying the Darcy's equation. After the routine measurements, porosity values were rounded to 1 decimal place and permeability values were rounded to 2 significant figures. The measurements of porosity and permeability were done at ALS Service PLC (Applied Petroleum Technology Ltd., UK).

RESULTS AND DISCUSSION

Lithofacies

The Antalo Limestone is laterally extensive covering the largest portion of the basin, with about 570 meters composite thickness measured from three outcrop locations namely; Giba-1 (270 m), Mesobo (175 m) and Chelekot (230 m) sections.

Giba-1 Section

The Giba-1 section is about 270 meters thick part of the Antalo Limestone, conformably overlies the Adigrat

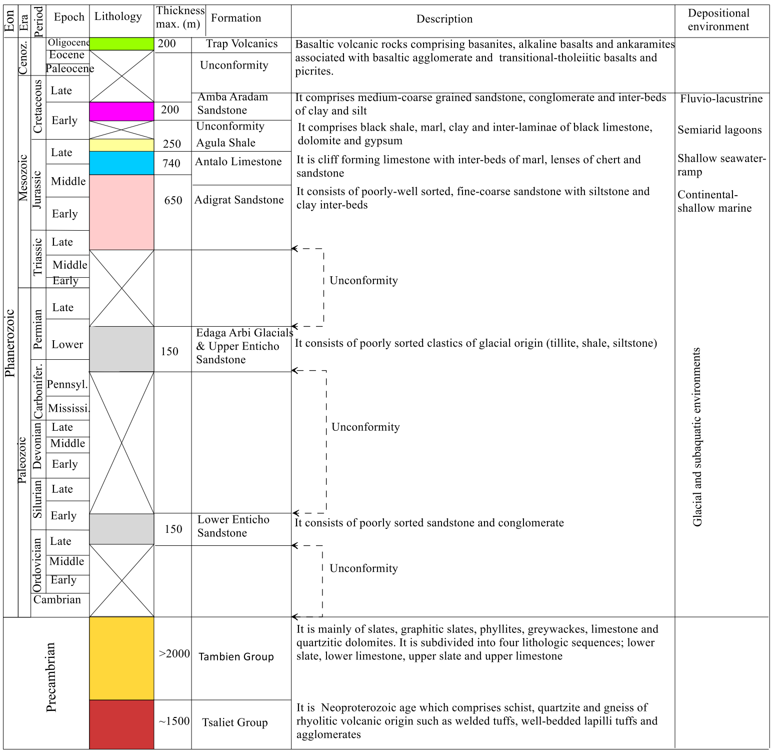

Figure 3: Composite stratigraphic section of the Mekelle Basin (After Beyth, 1972; Bosellini *et al.,* 1997).

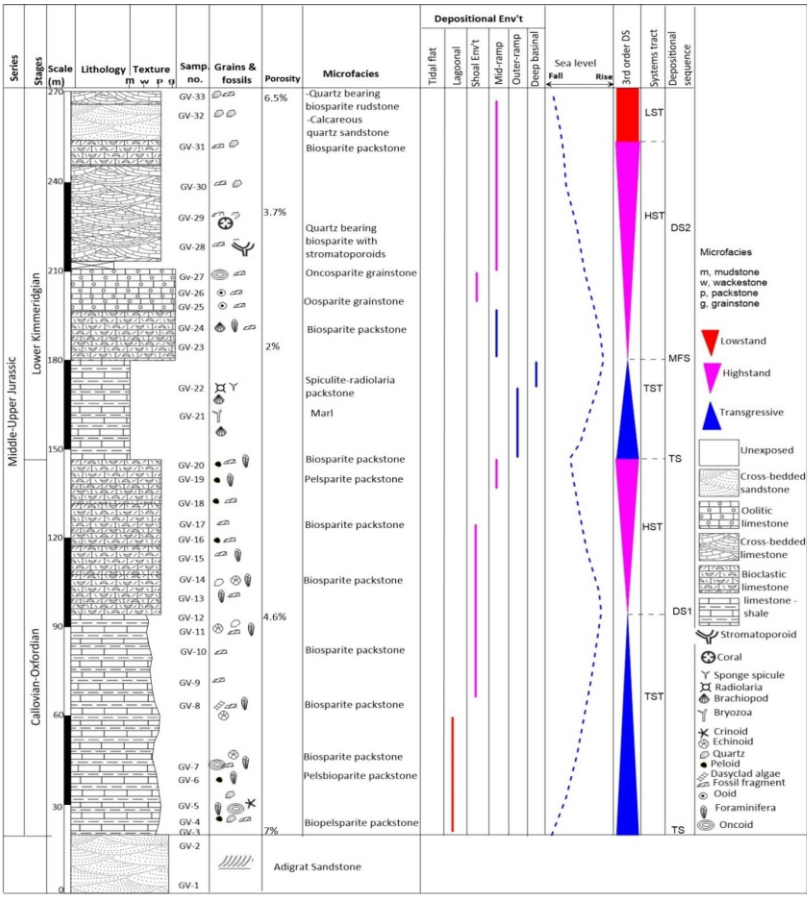

Figure 4: Sequence stratigraphic section of the Antalo Limestone at Giba-1 section, Mekelle Basin (Callovian – Lower Kimmeridgian)

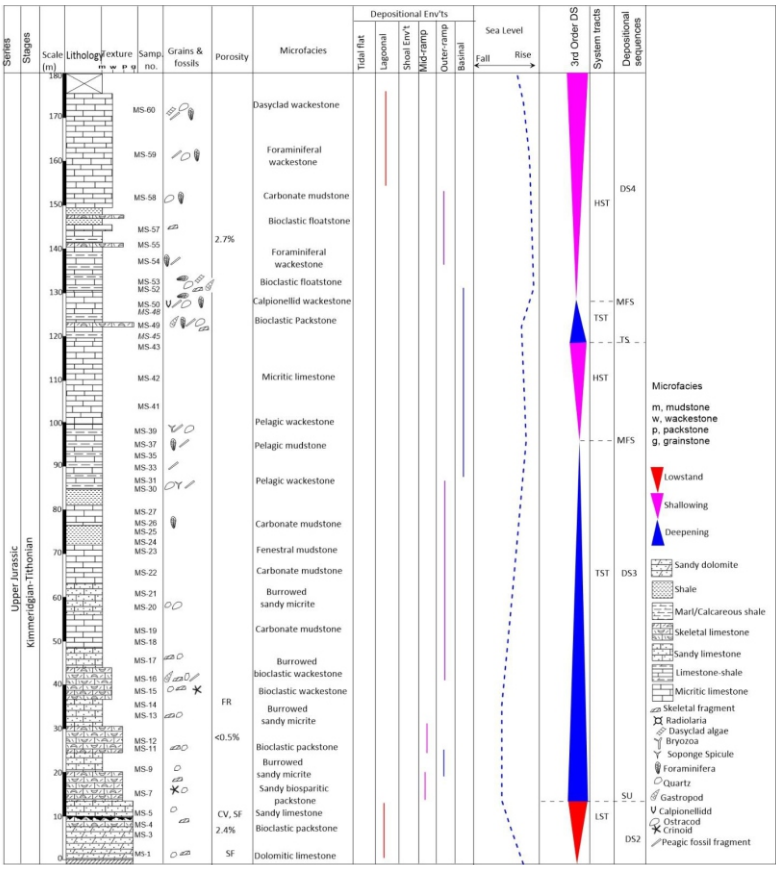

Figure 5: Sequence stratigraphic section of the Antalo Limestone at Mesobo section, Mekelle Basin (Kimmeridgian – Tithonian).

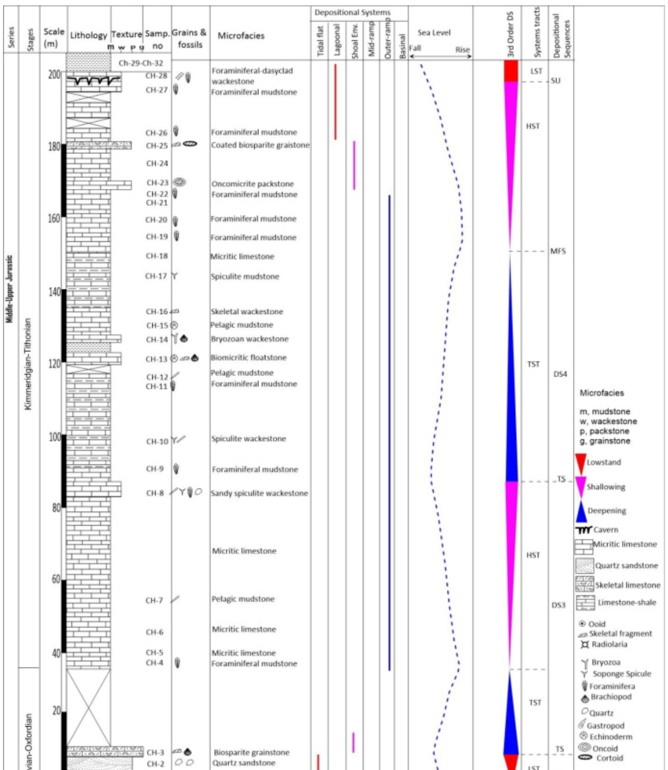

Figure 6: Sequence stratigraphic section of the Antalo Limestone at Chelekot section, Mekelle Basin (Callovian – Tithonian).

Sandstone (Figure 4). The lower 70 m thick part of the section, is characterized by gently sloping topography, comprising poorly exposed shale and limestone beds. The middlemost part of the section (90 – 145 m, samples GV-12 – GV-20), comprises very thick massive-well bedded cliff-forming limestone. The next~30 m thick part of the section (145 – 180 m), is characterized by a gentle topography, composed of dominantly marl and calcareous shale, with inter-bedded coquina and pelagic limestone (samples GV-21 and GV-22). The top part of the section (180 – 210 m), is a coarsening up succession comprising coarse carbonate grains (samples GV-23 – GV-27). The remaining uppermost part of the section (210 – 270 m), comprises thick beds of hummocky cross-bedded calcareous sandstone (GV-32) and hummocky cross-bedded limestone beds (samples GV-28 – GV-31 and GV-33).

Mesobo Section

The Mesobo section is a fault margin cliff-side exposure, which is found about 5 km north of the Mekelle Town. The total thickness of this section is about 175 meters (Figure 5). The dominant rock unit in this section, is limestone with subordinate shale layers. The lower 20 m thick part, samples MS-1 – MS-8, comprises beds of dolomitic limestone, sandy limestone and skeletal limestone characterized mainly by large scale karstic features; such as caves and caverns. The second subunit of this section (20 – 48 m, samples MS-9 – MS-17), is characterized by a cyclic stacking pattern of micritic and skeletal limestone beds. The overlying unit, is progressively changed to carbonate mudstone (48 – 63 m, samples MS-18 – MS-21). The carbonate mudstone, with progressively deepening facies, gray-black shale inter-beds and associated skeletal limestone beds, dominated the topmost part of the section (64 – 170 m, samples MS-22 – MS-60).

Chelekot Section

The Chelekot section represents about 230 meters thick part of the Antalo Limestone (Figure 6). The lower part, comprises sandstone bed at the bottom overlain by skeletal limestone. The next 50 m part of the section (10 – 35 m interval), is poorly exposed. The overlying 55 m thick part of the section (35 – 90 m, samples CH-4 – CH-9), is well exposed and comprised thickly bedded cliff-forming micritic limestone beds. The part of the section (95 – 150 m, samples CH-10 – CH-18) comprised poorly exposed shale and marl with inter-beds of micritic and skeletal limestone. The top 50 m part of the section (150 – 200 m, samples CH-19 – CH-29), comprised well-bedded micritic limestone facies with associated skeletal limestone beds. The topmost part of this section exhibits networks of cavernous porosity.

Generally, the different lithofacies types identified and described in these sections (Giba-1, Mesobo and Chelekot), with thickness measurements and sampling included shale, sandstone, fossiliferous limestone, cavernous limestone, horizontally well-bedded to massive fine-grained limestones, containing condensed sections (Figure 7).

Microfacies

From the analyzed 92 samples, different microfacies types; such as carbonate mudstone, wackestone, packstone, grainstone, dolomitic and sandy limestone were identified, of which 18 representative samples have been described, with environmental interpretations (Table 1).

Diagenesis

The role of diagenesis is critical, in controlling the reservoir qualities of carbonate rocks; creates new pore spaces and enhance the available porosity of reservoirs, through dissolution and fracturing or reduce and destroy the original depositional porosity through mechanical compaction and cementation (Moore, 1989). In this study, the dominant diagenetic changes identified from all sections include; cementations and partly compaction, that destroyed the original depositional porosities. These diagenetic changes have been well discussed in (Adefris et al. (2020). However, there are evidence of meteoric dissolution; such as caverns, caves, solution enlarged fractures, molds and vugs.

The coarse grained microfacies, comprised oosparite, oncosparite and pelsparite grainstones, which showed different diagenetic features. The oosparite grainstone is a well-sorted and mud-free grain-supported microfacies, comprising about 75 – 80% ooids and 10 – 12% sparry calcite cement, with few monocrystalline quartz grains, representing 2 – 3% of the sample (Figure 8A). The associated skeletal fragments represent mainly crinoid fragments (8 – 10%). This microfacies was identified from Giba-1 section (samples GV-25 and GV-26).

The oncosparite grainstone comprised about 80% coarse sand-sized (0.8 – 1 mm in diameter), sub-spheroidal-ellipsoidal, well-sorted, and well-rounded micritic oncoids (Figure 8B). There are about 5% skeletal fragments, comprising shells of echinoid (<1mm length), gastropods, and corals. These grains are highly compacted, creating a linear to concavo-convex grain contacts, as manifested by deformed grain-grain contact areas. The intergranular pore spaces are filled by coarse blocky calcite cement (15%). This microfacies was identified from the Giba-1 section (sample GV-27), associated with oolitic limestone beds. The occurrence of pore-filling fine to coarse calcite crystals in these microfacies, indicates meteoric to marine phreatic cementations (Longman, 1980; Moore, 1989; Mazzullo and Chilingarian, 1992).

Well-sorted, fine sand-sized (0.15 – 0.2 mm in diameter), spherical and rounded micritic peloid grains, make up

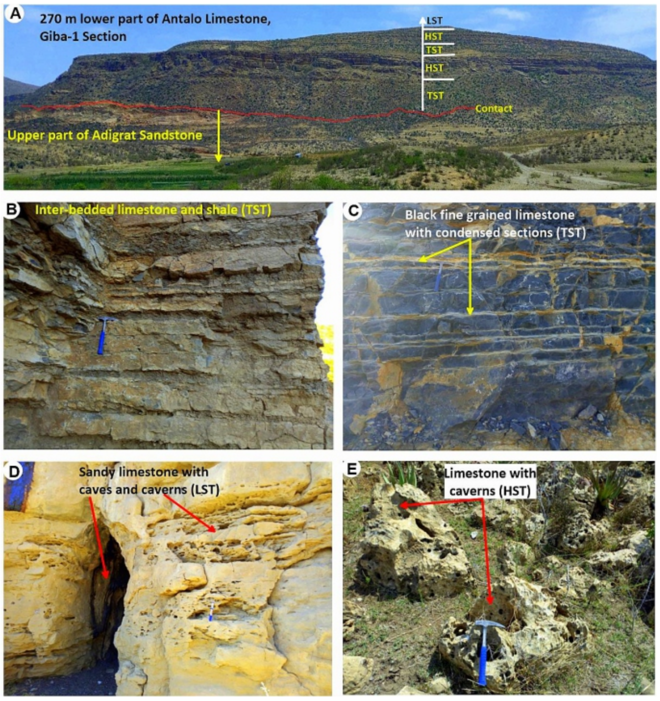

Figure 7: Different lithofacies types: A. 270 meters lower part of Antalo Limestone at Giba-1 section, B. Micritic limestone beds with inter-bedded shale layers (Mesobo section, 84 – 91 m interval, samples MS-30 – MS-35), C. Bedded black micritic limestone (pelagic) with condensed sections (Mesobo section, 127 – 132 m interval, samples MS-50 – MS-53), D. Caves and caverns in sandy limestone (Mesobo section, 8 – 13 m interval, samples MS-3 – MS-5), E. Cavernous limestone (Chelekot section, 195 – 200 m interval, samples CH-27 – CH-28). TST, Transgressive Systems Tract; HST, Highstand Systems Tract; LST, Lowstand Systems Tract.

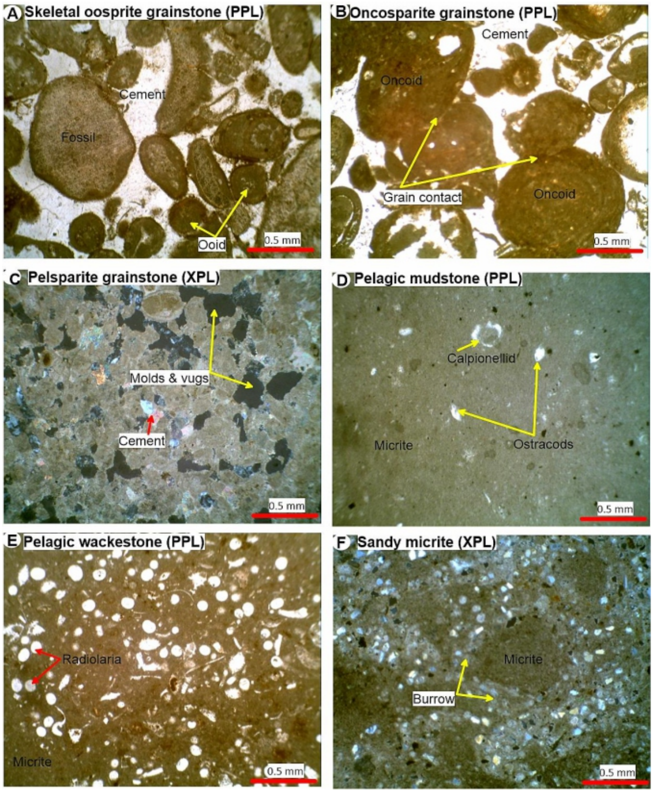

Figure 8: Different microfacies types: A. Well-cemented oosparite grainstone (Giba-1 section, sample GV-26), B. Well-cemented oncosparite grainstone (Giba-1 section, sample GV-27), C. Pelsparite grainstone, with moldic and vuggy porosities (Chelekot section, sample CH-29), D. Pelagic mudstone, comprising calpionellids, ostracods and sponge spicules (Mesobo section, sample MS-50), E. Pelagic wackestone, comprising mainly radiolarian and sponge spicules (Giba-1 section, sample GV-22), F.

Table 1: Petrographic description of some selected samples from Giba-1, Mesobo and Chelekot sections.

Location	**Sample No.**	**Petrographic data**									**Depositional environment** (Wilson, 1975; Flügel, 2004)
		Allochems %				Micrite %	Cement %	Quartz %	Porosity %	Microfacies	
		Fossil	Ooid	Oncoid	Peloid						
Giba-1	GV-6	15			5	35	45			Pelbiosparite packstone	Lagoonal
	GV-15	20				30	50			Biosparite packstone	Sand shoal
	GV-22	15				85				Pelagic wackestone	Deep basinal
	GV-25	8	80				10	2		Oosparite grainstone	Sand shoal
	GV-26	10	75				12	3		Oosparite grainstone	Sand shoal
	GV-27	5		80			15			Oncosparite grainstone	Sand shoal
Mesobo	MS-1					10	81 % dolomite	3	6	Dolomitic limestone	Tidal flat
	MS-5					10	66	15	9	Sandy limestone	Tidal flat
	MS-14					80		20		Sandy micrite	Outer-ramp
	MS-39	40				60				Pelagic wackestone	Deep basinal
	MS-42					100				Carbonate mudstone	Deep basinal
	MS-50	2				98				Pelagic mudstone	Deep basinal
	MS-60	15				90				Dasyclad wackestone	Lagonal
Chelekot	CH-2						10	90		Calcareous sandstone	Tidal channel
	CH-12	7				92		1		Pelagic mudstone	Outer-ramp – deep basinal
	CH-25	30				15	55			Biosparite grainstone	Sand shoal – lagoonal
	CH-28	15				85				Biomicrite wackestone	Lagoonal
	CH-29				85		5		10	Pelsparite grainstone	Lagoonal

about 85% of the pelsparite grainstone, with about 5% drusy calcite cements and 10% vuggy and moldic pores (Figure 8C). This shows that dissolution is important process affecting some parts of the Antalo Limestone, in creating vugs, molds, and solution-enlarged fractures. This microfacies was identified from the top part of Chelekot section (sample CH-29).

There are pelagic limestones, with very fine, dense, homogeneous micrite matrix, comprising pelagic microfossils; such as ostracods, calpionellids, radiolarian and sponge spicules (Figure 8D, E). These microfacies were identified from the Giba-1 (sample GV-22) and Mesobo (sample MS-50) sections. The other carbonate mudstone facies represent burrowed sandy micrite, and composed of micrite matrix (80%), with very fine microsparite and significant amounts of quartz grains (20%). Patches of circular swirls/fabrics, made up of fine sand-sized, sub-angular to rounded quartz grains within micrite, characterized this microfacies (Figure 8F). It was identified from the Mesobo section (sample MS-14). The occurrences of burrows represent hardgrounds, created due to the precipitation of microcrystalline calcite crystals (Pemberton *et al.,* 1992; Boggs 2006). This type of cementation occur during peak sea-level conditions, creating phases of nondeposition and leading to the precipitation of fine calcite crystals (Christ *et al.,* 2015).

Dolomitization is less contributing to the diagenetic evolution of the Antalo Limestone, as confirmed with the rare occurrence of dolomite crystals in the studied samples. However, crystals of dolomite rhombohedra were identified from the Mesobo section (sample MS-1). The dolomitic limestone is quartz-bearing and composed of fine-grained (0.15 mm), equigranular, cloudy dolomite crystals, with some well-developed rhomboid shape (Figure 9 A, B). However, most of the crystals have crudely developed crystal shape, with the associated relicts of microcrystalline carbonate mud along grain boundaries. It comprises about 3% subangular to rounded, medium to coarse grained (0.2 – 0.7 mm), monocrystalline quartz crystals exhibiting undulated extinction. It also comprises solution-enlarged fracture porosity (6%). The rhombohedral crystals represent dolomite crystal growths and gradual replacement of the original calcite by low-magnesian calcite, precipitated from meteoric fluids as a result of subaerial exposure (Mazzullo and Chilingarian, 19 92).

There is also sandy limestone, made up of very fine calcite spars and micrite (76%) and quartz grains (15%), with karst features including channel porosities (9%) (Figure 9 C, D). The quartz grains are fine-medium sand sized (0.1 – 0.3 mm), angular-sub rounded, well sorted and highly fractured. Micrite occurs as relict embedded within the calcite crystals. These facies were identified from the Mesobo section (sample MS-5).

Sandy micrite, with burrows (Mesobo section, sample MS-14). PPL, Plane Polarized Light; XPL, Crossed Polarized Light.

Sequence stratigraphy

Based on the stratal stacking patterns and the identified sequence stratigraphic boundaries, the Callovian – Tithonian Antalo Limestone of the Mekelle Basin has been subdivided into four (4) third-order depositional sequences; DS1, DS2, DS3, and DS4, plus nine (9) systems tracts (Figure 10). These third-order sequences are the results of short-term cyclic global sea-level changes that span 1 to 5 million years (Vail *et al.,* 1977; Haq *et al.,* 1987). The identified sequences stratigraphic boundaries include; subaerial unconformities, transgressive and maximum flooding surfaces. Transgressive surfaces (TS) were recognized from deepening upward facies changes. Subaerial unconformities (SU) were recognized from evidences of exposure and the subsequent dissolutions such as caves, caverns, vugs, molds and solution-enlarged porosities associated with dolomite facies. Maximum flooding surfaces (MFS) were recognized from condensed sections and microfacies comprising assemblages of pelagic microfossils.

Depositional sequence 1 (Ds1)

The first depositional sequence (DS1) represents the lower part of the Antalo Limestone (Callovian – Oxfordian), which conformably overlies the Adigrat Sandstone. Two systems tracts namely; TST and HST were identified in DS1 depositional sequence. The TST comprised shale-limestone intercalation at the bottom. The limestone beds comprised foraminifera-bearing wackestone/packstone microfacies, interpreted as deposited in lagoonal environments (Tucker and Wright 1990; Hughes, 2004). The HST is a mid-ramp to sand shoal deposit, comprising dominantly skeletal packstone/grainstone microfacies, with pore-filling meteoric phreatic drusy calcite cement destroying the original intergranular pore spaces. DS1 corresponds to the first member (Jta) of Beyth (1972) and the transitional beds and depositional sequence A1 of Bosellini *et al.* (1997).

Depositional sequence 2 (Ds2)

The second depositional sequence (Upper Oxfordian – Lower Kimmeridgian) comprised three vertically stacked systems tracts; TST, HST, and LST. The TST is characterized by marly units, with coquina inter-beds and abundant brachiopod and inter-beds of pelagic limestones. The pelagic microfacies are deep basinal (Scholle et al., 1983), that indicate maximum sea-level conditions and the maximum flooding surfaces. The middle part of DS2 is dominated by thick beds of sand bars, composed of skeletal fragments, ooids, and oncoids. Meteoric phreatic to marine cement that filled the inter-

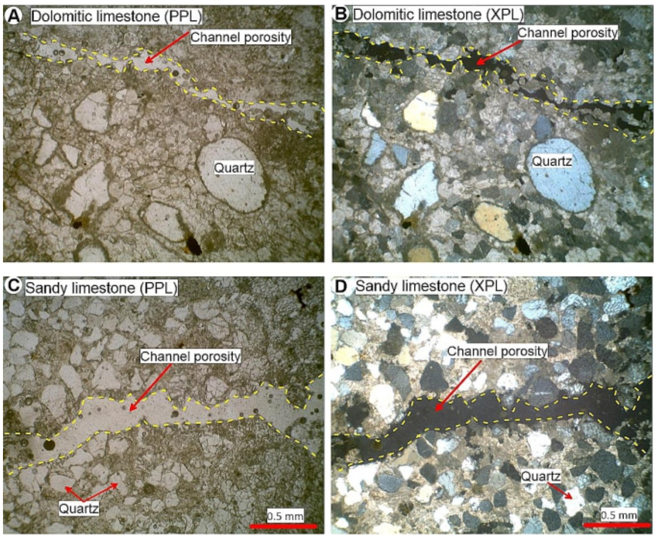

Figure 9: Dolomitic limestone (A – B, sample MS-1) and sandy limestone (C – D, sample MS-5) microfacies, with solution-enlarged fractures/channel porosities, Mesobo section. PPL, Plane Polarized Light; XPL, Crossed Polarized Light.

Table 2: Core-plug porosity-permeability data.

Sample no.	Location	Sample type	Systems tract	Depositional sequence	Helium porosity (%)	Air permeability (mD)
GV-3	Giba-1	Limestone	TST	DS1	4.8	0.08
GV-12	Giba-1	Limestone	HST	DS1	4.6	<0.01
GV-23	Giba-1	Limestone	HST	DS2	2.0	<0.01
GV-29	Giba-1	Limestone	HST	DS2	3.7	<0.01
GV-33	Giba-1	Limestone	LST	DS2	6.5	0.91
MS-3	Mesobo	Limestone	LST	DS2	2.4	<0.01
MS-12	Mesobo	Limestone	TST	DS3	<0.5	<0.01
MS-55	Mesobo	Limestone	HST	DS4	2.7	<0.01

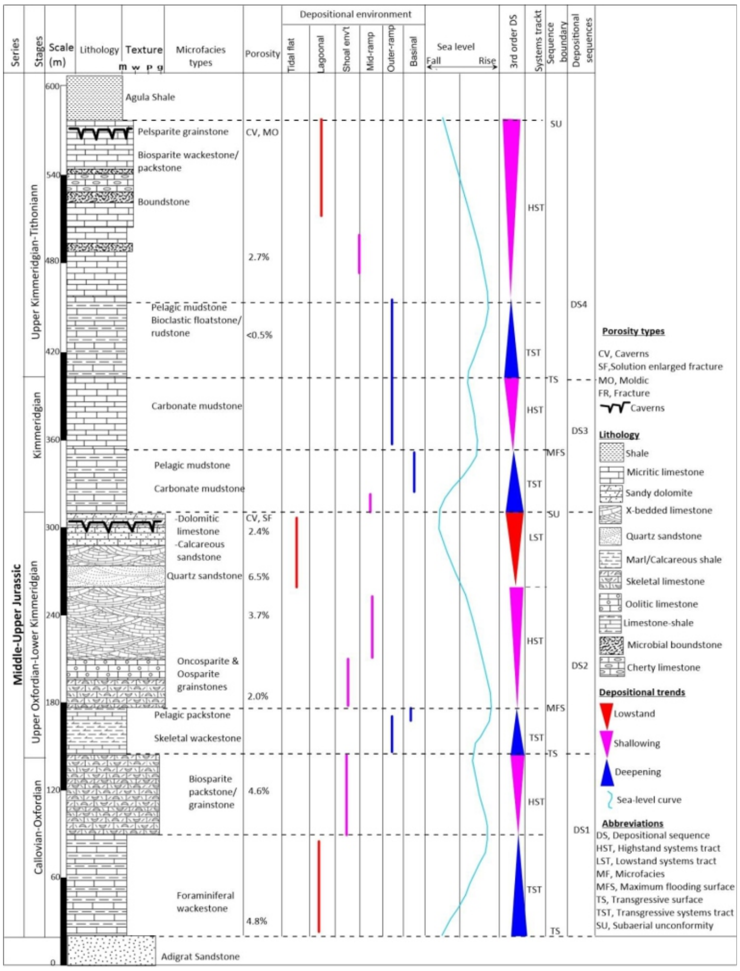

Figure 10: Composite sequence stratigraphic section of the Antalo Limestone comprising four third-order depositional sequences (DS), systems tracts (TST, HST, and LST) and sequence boundaries (SU, TS and MFS)

granular pore spaces, is the second major component of these microfacies. This is a sand shoal deposit of the inner-ramp setting (Wilson, 1975; Flugel, 2004), representing highstand systems tract (HST). The cavernous sandy limestone and dolomitic limestone, with solution-enlarged fracture porosities are indicators of subaerial exposure and subsequent meteoric diagenesis (dolomitization and dissolution), in tidal flat environment during relative sea-level fall under humid climatic conditions (Tucker,1993). This represents lowstand systems tract (LST) and the subaerial unconformity was inferred from the dolomitic limestone and the associated cavernous and channel pores. DS2 corresponds to the second member (Jtb) of Beyth (1972) and depositional sequence A2 of Bosellini *et al.* (1997).

Depositional sequence 3 (Ds3)

The third depositional sequence comprised mid-ramp to deep basinal facies, representing TST and HST (Kimmeridgian). The TST is characterized by thin beds of limestone, with inter-layers of gray-black shale. The limestone beds comprised burrowed sandy micrite, biosparitic packstone, carbonate mudstone, and pelagic wackestone microfacies. Marine cementation indicated by lithified hardgrounds and microcrystalline sparry calcite cement of marine origin (Taylor and Wison, 2003), is also the characteristic features of this systems tract. The hardgrounds represent a drowning unconformity, created due to rapid relative sea-level rise during transgression that created accommodation spaces and insufficient sediment production, and ultimately leads to non-deposition (Jones and Desrochers, 1992). The top part of the TST comprises thin layers of pelagic limestones, with associated siltstone layers. The limestone beds are composed of abundant fine fragments of pelagic microfossils, ostracods, and sponge spicules, which are the results of deposition in deep basinal environments, indicating maximum sea-level and maximum flooding surfaces (Scholle et al., 1983); Hughes 2000).

The HST is composed of very thick, massively bedded, light-yellow, blue-black, gray, and very fine carbonate mudstone. There is no sign of pro-gradational depositional trend rather it showed aggradational pattern, which was deposited when the rate of sedimentation and accommodation were balanced (Nichols, 2009). DS3 corresponds to the third member (Jtc) and the lower part of the fourth member (Jtd) of Beyth (1972) and depositional sequence A3 of Bosellini *et al.* (1997).

Depositional sequence 4 (Ds4)

The fourth depositional sequence represents the topmost part of the studied sections (Upper Kimmeridgian – Tithonian), comprising two systems tracts namely; TST and HST. The TST comprised gray-black shale layers, thin micritic, and coquina inter-beds, with relatively thick pelagic limestone beds, characterized by thin streaks of mud (condensed sections). The HST is very thick cliff-forming part of the unit, which comprises foraminifera-bearing carbonate mudstone beds, skeletal wackestone, and pelsparite grainstone. The topmost part of HST is characterized by karstic features, created due to meteoric diagenesis, which took place during sea-level lowstand (Tucker, 1993). This is the second subaerial unconformity identified within the unit and considered as the top sequence boundary. DS4 corresponds to the top part of the fourth member (Jtd) and the fifth member (Jte) of Beyth (1972) and depositional sequence A4 of Bosellini *et al*., (1997).

Direct porosity-permeability measurements

The analyzed samples show very low porosity and permeability values (Table 2). All samples selected from the transgressive systems tract (characterized by mud-supported fabric) and highstand systems tract (characterized by fully cemented intergranular pores), have porosity ranging from 0.5% to 4.8% and 0.01 – 0.08 mD permeability. A sample from the lowstand systems tract (characterized by grain-supported fabric and vuggy and moldic pores), has 6.5% porosity with 0.91 mD permeability. Porosity values below 5% and permeability values below 1 mD, generally indicate poor reservoir quality (Robinson, 1966; Ahr, 2008). On the other hand, the sample, with 6.5% porosity show some capacity of storing fluid, but it is still considered as poor-quality reservoirs since its permeability value is very low (Ahr, 2008).

Reservoir potential

From the combined analyses of diagenetic features and sequence stratigraphic frameworks; dissolution porosities such as caves, caverns, vugs, molds, and solution-enlarged fractures, possibly with high permeability, have been identified in the lowstand systems tract (LST) of the second depositional sequence (DS2) and highstand systems tract (HST) of the fourth depositional sequence (Ds4). These systems tracts are considered to have some potential for reservoir in the Antalo Limestone, Mekelle Basin.

CONCLUSIONS

Based on lithofacies evidences, microfacies, facies stacking patterns and the identified sequence boundaries, Antalo Limestone has been subdivided into four third-order depositional sequences (DS) and nine systems tracts. The most significant and prevailing diagenetic process that destroyed the original depositional porosities is cementation. Dissolution played a significant role, in creating caves, caverns, solution-enlarged fracture porosities, vugs, and molds. These features were identified from the lowstand systems tract (LST) of the second depositional sequence (DS2) and the highstand systems tract (HST) of the fourth depositional sequence

(Ds4), indicating the presence of potential reservoir beds. Therefore, Antalo Limestone in the Mekelle Basin is considered to have some potential for reservoir.

REFERENCES CITED

Adefris, D., Nton, M. E., Boboye, O. A., Atnafu, B. (2020): Petrography and stable oxygen and carbon isotopic composition of the Antalo Limestone, Mekelle Basin, Northern Ethiopia: Implications for the marine environment and deep-burial diagenesis. Carbonates and Evaporites, Accepted m, pp. 1-17, https://doi.org/10.1007/s13146-020-00659-5.

Ahr, W. M. (2008): Geology of Carbonate Reservoirs - The Identification, Description, and Characterization of Hydrocarbon Reservoirs in Carbonate Rocks. John Wiley and Sons: New Jersey, 277 p.

Alemu, T., Abdelsalam, M.G., Dawit, E.L., Atnafu, B., Mickus, K.L. (2018): The Paleozoic-Mesozoic Mekele Sedimentary Basin in Ethiopia: An example of an exhumed Intracontinental Sag (ICONS) basin. Journal of African Earth Sciences, 143, pp. 40-58, https://doi.org/10.1016/j.jafrearsci.2018.03.010.

Arkin, Y., Beyth, M., Dow, D. B., Levitte, D., Haile, T., Hailu, T. (1971): Geological Map of Mekele Sheet Area ND 37-11, Tigre Province. Geological Survey of Ethiopia: Addis Ababa, 1 p.

Ayalew, D., Yirgu, G. (2003): Crustal contribution to the genesis of Ethiopian plateau rhyolitic ignimbrites?: basalt and rhyolite geochemical provinciality. Journal of the Geological Society of London, 160, pp. 47-56, https://doi.org/10.1144/0016-764901-169.

Beyth, M. (1972): Paleozoic-Mesozoic Sedimentary Basin of Mekele Outlier, Northern Ethiopia. AAPG Bulletin, 56(12), pp. 2426-2439, https://doi.org/10.1306/819A422A-16C5-11D7-8645000102C1865D.

Beyth, M., Avigad, D., Wetzel, H., Matthews, A., Berhe, S. M. (2003): Crustal exhumation and indications for Snowball Earth in the East African Orogen: north Ethiopia and east Eritrea. Precambrian Research, 123, pp. 187-201, https://doi.org/10.1016/S0301-9268(03)00067-6.

Boggs, S. J. (2006): Principles of Sedimentology and Stratigraphy. Pearson Prentice Hall: New Jersey, 662 p.

Bosellini, A., Russo, A., Fantozzi, P.L., Assefa, G., Solomon, T. (1997): The Mesozoic Succession of the Mekele Outlier (Tigre Province, Ethiopia). Memorie di Scienze Geologiche, 49, pp. 95-116.

Bosellini, A., Russo, A., Assefa, G. (2001): The Mesozoic succession of Dire Dawa, Harar Province, Ethiopia. Journal of African Earth Sciences, 32(3), pp. 403-417.

Bussert, R. (2010): Exhumed erosional landforms of the Late Palaeozoic glaciation in northern Ethiopia: Indicators of ice-flow direction, palaeolandscape and regional ice dynamics. Gondwana Research, 18, pp. 356-369, https://doi.org/10.1016/j.gr.2009.10.009.

Bussert, R., Schrank, E. (2007): Palynological evidence for a latest Carboniferous-Early Permian glaciation in Northern Ethiopia. Journal of African Earth Sciences, 49, pp. 201-210, https://doi.org/10.1016/j.jafrearsci.2007.09.003.

Carrigan, W.J., Cole, G.A., Colling, E.L., Jones, P.J. (1995): Geochemistry of the Upper Jurassic Tuwaiq Mountain and Hanifa Formation Petroleum Source Rocks of Eastern Saudi Arabia. In: Petroleum Source Rocks, Katz, B.J. (ed.),. Springer-Verlag, Berlin, pp. 67-87.

Catuneanu, O. (2006): Principles of Sequence Stratigraphy. Elsevier B.V: Amsterdam-Boston, 375 p.

Christ, N., Immenhauser, A., Wood, R., Darwich, K., Niedermayr, A. (2015): Petrography and environmental controls on the formation of Phanerozoic marine carbonate hardgrounds. Earth Science Reviews, pp. 1-129, https://doi.org/10.1016/j.earscirev.2015.10.002.

Ehrenberg, S.N., Nadeau, P.H. (2005): Sandstone vs. Carbonate petroleum reservoirs - A global perspective on porosity-depth and porosity-permeability relationships. AAPG Bulletin, 89(4), pp. 435-445, https://doi.org/10.1306/11230404071.

EMoM. (2011): Petroleum Exploration in Ethiopia - Information and Opportunities. Unpublished Report, Ethiopian Ministry of Mines, Addis Ababa, pp. 1-20.

Flügel, E. (2004): Microfacies of Carbonate Rocks: Analysis, Interpretation and Application. Springer: Erlangen, 976 p.

Gani, N.D.S., Abdelsalam, M.G., Gera, S., Gani, M.R. (2008): Stratigraphic and structural evolution of the Blue Nile Basin, Northwestern Ethiopian Plateau. Geological Journal, pp. 1-27. https://doi.org/10.1002/gj

Getaneh, W., Valera, R. (2002): Rare earth element geochemistry of the Antalo Supersequence in the Mekele Outlier (Tigray region, northern Ethiopia). Chemical Geology, 182, pp. 395-407.

Hakimi, M.H., Abdullah, W.H., Shalaby, M.R. (2010): Organic geochemistry and thermal maturity of the Madbi Formation, East Shabowah Oil fields, Masila Basin, Yemen. Bulletin of the Geological Society of Malaysia, 56, pp. 41-48.

Hakimi, Mohammed Hail, Abdullah, W.H., Shalaby, M.R. (2012): Madbi-Biyadh/Qishn (!) petroleum system in the onshore Masila Basin of the Eastern Yemen. Marine and Petroleum Geology, 35, pp. 116-127, https://doi.org/10.1016/j.marpetgeo.2012.01.009.

Haq, B. V., Hardenbol, J., Vail, P. R. (1987): The chronology of fluctuating sea level since the Triassic. Science, 26, pp. 483-489.

Hughes, G. (2004): Middle to Upper Jurassic Saudi Arabian carbonate petroleum reservoirs: biostratigraphy, micropalaeontology and palaeoenvironments. GeoArabia, 9(3), pp. 79-114.

Hughes, G. (2000): Saudi Arabian Late Jurassic and Early Cretaceous agglutinated foraminiferal associations and their application for age, palaeoenvironmental interpretation, sequence stratigraphy, and carbonate reservoir architecture. In: Proceedings of the Fifth International Workshop on Agglutinated Foraminifera, Hart, M.B., Kaminski, M.A., Smart, C.W. (eds.), Grzybowski Foundation Special Publication, pp. 149-165.

Hunegnaw, A., Sage, L., Gonnard, R. (1998): Hydrocarbon Potential of the Intracratonic Ogaden Basin, SE Ethiopia. Journal of Petroleum Geology, 21(4), pp. 401-425.

Jones, B., Desrochers, A. (1992): Shallow Platform Carbonates. In: Facies Models Response to Sea Level Change, Walker, R.G., James, N.P. (eds.), Geological Association of Canada, pp. 277-302.

Kabeto, K. (2010): Geological and geochemical variations in Mid-Tertiary Ethiopian Flood Basalt Province, Maychew, Tigray Region, Ethiopia. MEJS, 2(1), pp. 4-25.

Kiessling, W., Pandey, D.K., Schemm-gregory, M., Newis, H., Aberhan, M. (2011): Marine benthic invertebrates from the Upper Jurassic of northern Ethiopia and their biogeographic affinities. Journal of African Earth Sciences, 59, pp. 195-214, https://doi.org/10.1016/j.jafrearsci.2010.10.006

Mazzullo, S. J., Chilingarian, G. V. (1992): Diagenesis and Origin of Porosity. In: Carbonate reservoir characterization - a geologic-engineering analysis, part I - Developments in Petroleum Science, Chilingarian, G.V., Mazzullo, S.J., Rieke, H.H. (eds.), Elsevier Scientific Publishers B. V., pp. 199-270.

Merla, G., Minucci, R. (1938): Missione geologica nel Tigrai. vol. 1" La Serie dei Terreni". Regia Accademia d'Italia, Rome, 362 p.

Miall, A.D. (2010): The Geology of Stratigraphic Sequences. Springer-Verlag: Dordrecht, 522 p.

Moore, C.H. (1989): Carbonate Diagenesis and Porosity: Developments in Sedimentology 46. Elsevier Science B. V: Amsterdam, 338 p.

Nichols, G. (2009): Sedimentology and Stratigraphy (Second ed.). John Wiley and Sons: Chichester, 419 p.

Pemberton, S.G., MacEachem, J.A., Frey, R.W. (1992): Trace fossil facies models- environmental and allostratigraphic significance. In: Facies Models Response to Sea Level Change, Walker, R.G., James, N.P. (eds.), Geological Association of Canada, pp. 47-72.

Russo, A., Assefa, G., Atnafu, B. (1994): Sedimentary evolution of the Abay River (Blue Nile) Basin, Ethiopia. Neues Jahrbuch Für Geologie Und Paläontologie, 5, pp. 291-308.

Scholle, P. A., Arthur, M. A., Ekdale, A. A. (1983): Pelagic Evironment. In: Carbonate Depositional Environments, Scholle, P.A., Bebout, D.G., Moore, C.H. (eds.), AAPG/Datapages, pp. 619-691.

Taylor, P.D., Wilson, M.A. (2003): Palaeoecology and evolution of marine hard substrate communities. Earth Science Reviews, 62, pp. 1-103, https://doi.org/10.1016/S0012-8252(02)00131-9.

Tefera, M., Chernet, T., Haro, W. (1996): Explanation of the Geological Map of Ethiopia. Ethiopian Institute of Geological Survey: Addis Ababa, 79 p.

Tucker, M. (1993): Carbonate diagenesis and sequence stratigraphy. In: Sedimentology Review/1, Wright, V.P (ed.), Blackwell Scientific Publications, Oxford, pp. 51-72.

Tucker, M. E., Wright, V. P. (1990): Carbonate Sedimentology. Blackwell Science: Oxford, 482 p.

Vail, P.R., Mitchum, R.M., Todd, R.G., Widmeir, J.M., Thompson S., Sangree, J.B., Bubb, J.N., Hatlelid, W.G. (1977): Seismic stratigraphy and global changes of sea level. In: Seismic Stratigraphy-Applications to Hydrocarbon Exploration Payton, C.E. (ed.), AAPG/Datapages, pp. 49-212.

Wilson, J.L. (1975): Carbonate Facies in Geologic History. Springer-Verlag: Berlin, 471 p.

Worku, T., Astin, T.R. (1992): The Karoo sediments (Late Palaeozoic to Early Jurassic) of the Ogaden Basin, Ethiopia. Sedimentary Geology, 76, pp. 7-21.